Tetrahedron 66 (2010) 2875–2880

Contents lists available at ScienceDirect

Tetrahedron

journal homepage: www.elsevier.com/locate/tet

A theoretical investigation into chiral phosphoric acid-catalyzed asymmetric Friedel–Crafts reactions of nitroolefins and 4,7-dihydroindoles: reactivity and enantioselectivity

Chao Zheng, Yi-Fei Sheng, Yu-Xue Li *, Shu-Li You *

State Key Laboratory of Organometallic Chemistry, Shanghai Institute of Organic Chemistry, Chinese Academy of Sciences, 345 Lingling Lu, Shanghai 200032, China

ARTICLE INFO

Article history:
Received 16 November 2009
Received in revised form 3 February 2010
Accepted 5 February 2010
Available online 10 February 2010

Keywords:
Chiral phosphoric acid
Friedel–Crafts reaction
Enantioselectivity
Theoretical calculation
DFT

ABSTRACT

This article mainly focused on high level Density Functional Theory (DFT) studies on the chiral phosphoric acid-catalyzed Friedel–Crafts reactions between 4,7-dihydroindoles and nitroolefins. Firstly, the reactivities of 4,7-dihydroindole and indole in the chiral phosphoric acid-catalyzed Friedel–Crafts reactions with nitroolefin have been compared. The higher reactivity of 4,7-dihydroindole could be attributed to its higher HOMO energy as well as its more suitable trajectory to attack the nitroolefin in the transition state. Secondly, the origin of the enantioselectivity of the chiral phosphoric acid-catalyzed Friedel–Crafts reaction of 4,7-dihydroindole with nitroolefin has been studied using complete models on PBE1PBE/[6-311+G(d,p), 6-31G(d,p)] level. When (*S*)-**1b** was used as the catalyst, the enantioselectivity of the reaction is entirely controlled by the steric effect between the catalyst and the substrate. Whereas for catalyst (*S*)-**1c** the enantioselectivity is determined by the solvent effect.

1. Introduction

Chiral phosphoric acid has received much attention recently as powerful asymmetric organocatalyst.[1] Various reactions, such as Mannich-type,[2] Friedel–Crafts,[3] transfer hydrogenation,[4] hetero Diels–Alder[5] can be achieved efficiently using this catalyst system with high ees. These catalysts have also been successfully used in multi-component, cascade reactions[6] and in metal co-catalyzed reactions.[7] It was found in many cases that the chiral phosphoric acids are bifunctional catalysts bearing both Brønsted-acidic site and Lewis-basic site that activate two substrates simultaneously. Computational studies employing this type of catalytic model by Akiyama and Yamanaka et al.[8a] Goodman and Simón,[8b,c] Himo et al.,[8d,e] Yamanaka and Hirata,[8f] Shi and Song,[8g] and Ding and Li et al.[8h] on asymmetric transfer hydrogenation, Mannich, hydrophosphonylation and Baeyer–Villiger reaction provide good insights into the origin of enantioselectivities of these reactions. However, all these computational works focused on the reactions in which various imines were employed as the electrophile, while those reactions involving other electrophiles have still been untouched. On the other hand, high level computation with complete model has seldom been employed. In addition, as one of the most important type of carbon–carbon bond-formation reactions, the chiral phosphoric acid-catalyzed asymmetric Friedel–Crafts reaction has not been investigated with computational method.[9] The detailed mechanism of the chiral discrimination process is still unconfirmed despite that significant progress has been made in this field recently.

In 2008, Akiyama et al. reported a highly enantioselective Friedel–Crafts alkylation of indoles and nitroolefins (Scheme 1).[3h] (*R*)-BINOL derived chiral phosphoric acid **1a** was used as the catalyst. The reactions proceeded smoothly in benzene/1,2-dichloroethane (1:1) at −35 °C, with 10 mol % catalyst loading. For most substrates, (*R*)-products were obtained in excellent ees but with relatively long reaction time.

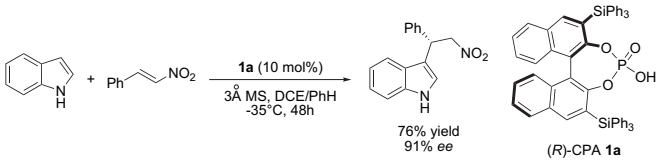

Scheme 1. Chiral phosphoric acid-catalyzed Friedel–Crafts reaction of indole with nitroolefin by Akiyama.[3h]

Subsequently, we[3j] demonstrated 4,7-dihydroindoles are also suitable in chiral phosphoric acid Friedel–Crafts alkylation reactions of nitroolefins. The Friedel–Crafts reaction together with a subsequent oxidation led to the 2-alkylated indoles in excellent yields

* Corresponding authors.
E-mail address: slyou@mail.sioc.ac.cn (S.-L. You).

0040-4020/$ – see front matter © 2010 Elsevier Ltd. All rights reserved.
doi:10.1016/j.tet.2010.02.031

and ees. A dramatic lifting of catalysis turn-over was observed for most substrates. With 10 mol % of the catalyst, reactions went to complete in minutes in benzene/dichloromethane (1:1) at room temperature. By adding the nitroolefin substrate slowly with syringe pump, the catalyst loading could be reduced to 0.5 mol %. When chiral phosphoric acid (*S*)-**1b** was used, the expected (*S*)-products were obtained with 41% ee. Interestingly, when the catalyst was changed to (*S*)-**1c**, the absolute configuration of the major product was reversed and (*R*)-products were produced with about 90% ee (Scheme 2). This is one of few reports[10] in which the configuration of the final products could be switched in chiral phosphoric-acid catalysis by changing 3,3′-substitution group on the catalyst.

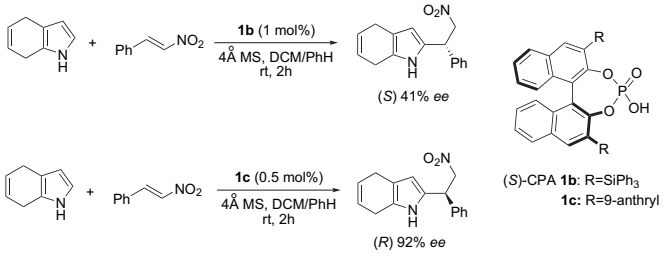

Scheme 2. Chiral phosphoric acid-catalyzed Friedel–Crafts reaction of 4,7-dihydroindole with nitroolefin by You group.[3j]

Intrigued by these experimental results, we began to use computational method to address (i) why 4,7-dihydroindole exhibits much higher reactivity than indole as the nucleophile in chiral phosphoric acid-catalyzed Friedel–Crafts reactions and (ii) how this unique enantioselectivity originates. Herein, we report our detailed computational studies.

2. Computational methods

Density Functional Theory (DFT) calculations were carried out with the Gaussian03 programs.[11] To compare the reactivities of indoles and 4,7-dihydrodinles in CPA-catalyzed Friedel–Crafts reactions, all the structures were located in gas phase with B3LYP[12] functional and 6-31G(d, p) basis set. Frequency analyses were performed to validate each structure being a minimum (without imaginary vibration) or a transition state (with only one imaginary vibration).

During the complete model study in 4,7-dihydroindole system, the PBE1PBE[13] functional was used instead of B3LYP. It has been well established that this functional usually gives good results in dealing with weak nonbonded interactions.[14] Both 6-31G(d, p) and 6-311+G(d, p) basis sets were used (vide infra). Frequency analyses were performed for all low-energy transition states. Solvent effects were considered by single point energy calculation using the IEFPCM[15] model (UAHF radii) in dichloromethane (ε=8.93) based on the optimized structures in gas phase.

Throughout this article, ΔE_{gas} and ΔG_{gas} denote the electronic energy and Gibbs free energy in gas phase, respectively. ΔG_{corr} denotes the solvent effect correction to the Gibbs free energy, ΔG_{sol} denotes the Gibbs free energy of the system in dichloromethane, and $-T\Delta S$ denotes the contribution of ΔS to the Gibbs free energy (T=298.15 K).

3. Results and discussion

3.1. The catalyst working model

Both Akiyama et al. and You et al. suggested that the chiral phosphoric acid acts as a bifunctional catalyst, in which the acid proton of the catalyst activates the nitroolefin while the phosphoryl oxygen atom forms hydrogen bond with the N–H moiety of the nucleophile. This type of arrangement results in 12-membered ring and 11-membered ring transition states in indole and dihydroindole systems, respectively (Fig. 1). These cyclic transition states are believed necessary for the high enantioselectivities of the Friedel–Crafts reactions.

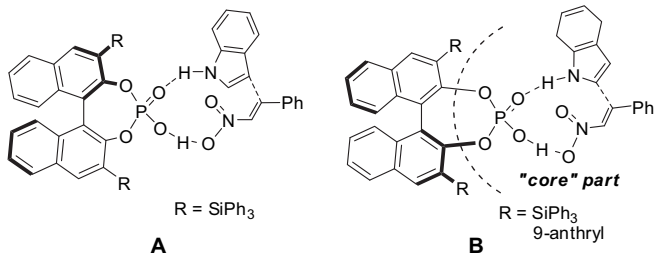

Figure 1. (A) 12-Membered ring TS in indole system. (B) 11-Membered ring TS in 4,7-dihydroindole system. For the complete models used to study the enantioselectivity in 4,7-dihydroindole system, two substrates, and the '*core*' part of the catalysts were described by 6-311+G(d, p) basis set while the BINOL skeleton and the R groups were described by 6-31G(d, p) basis set.

Unlike other electrophilic partners that are widely used in chiral phosphoric acid-catalyzed Friedel–Crafts reactions, such as imine[3a,d–g,i] or carbonyl[16], nitroolefins have more hydrogen bond receptors and therefore several different activation modes emerge in which hydrogen bond can be formed with the catalyst in different directions (Fig. 2). In addition, nitroolefin has one pro-chiral center, and nucleophile attacking from *Re*- or *Si*-face will afford (*R*)- or (*S*)-product, respectively. Although in both starting material and final product, the 2-position of 4,7-dihydroindole and the 3-position of indole are not a chiral center, however, in the electrophilic attacking step, there is a facial-selective issue.

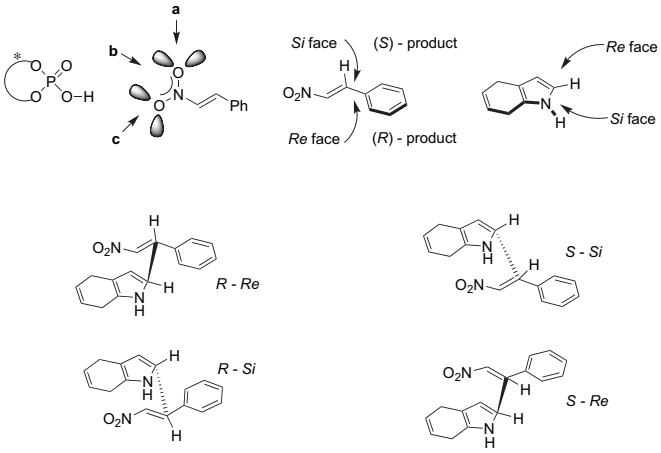

Figure 2. Possible activation and reaction modes.

3.2. The reactivities of 4,7-dihydroindole and indole

It is generally accepted that the nucleophilic attack of the aromatic ring to the electrophilic partner is the rate-determining step (RDS) in the Friedel–Crafts reaction.[17] The following proton transfer is a fast process. In order to compare the reactivities of 4,7-dihydroindole and indole, the rate-determining steps were studied with a simplified biphenyl-derived phosphoric acid (Fig. 3). Based on a conformational search (See Supplementary data for detail), the most stable structures of **TS-A** and **TS-B** are located and shown in Figure 4. The sum of the Gibbs free energies of the catalyst and the two substrates are used as the zero point reference. In the indole system, the Gibbs free energy of **TS-B** is 24.2 kcal/mol, whereas for 4,7-dihydroindole, the energy barrier is much lower (19.4 kcal/mol), indicating much higher reactivity, which corresponds well with the experiments.

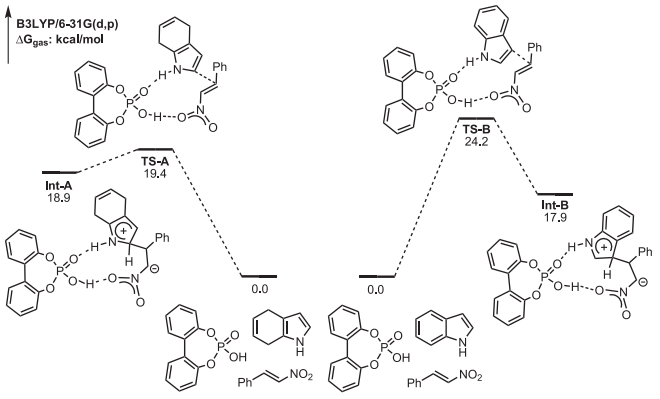

Figure 3. The reaction profiles of the rate-determining step of the Friedel–Crafts reactions of nitroolefin with 4,7-dihydroindole and indole. The relative Gibbs free energies in gas phase (ΔG_{gas}) are in kcal/mol. Calculated on B3LYP/6-31G(d, p) level of theory.

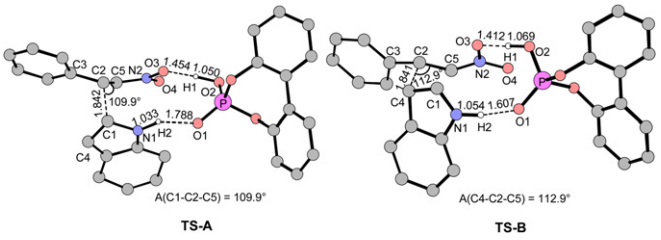

Figure 4. The optimized structures of transition states **TS-A** and **TS-B**. Most hydrogen atoms are omitted for clarity. Distances are in angstrom, angles are in degree. Calculated on B3LYP/6-31G(d, p) level of theory.

We next compared the energies of the Frontier Molecular Orbitals (FMO) of all substrates. The energies of the HOMO of 4,7-dihydrodindole and indole are −4.4 eV and −4.6 eV, respectively, and the energy of the LUMO of (*E*)-(2-nitrovinyl)benzene is −2.2 eV. The energy of the HOMO of 4,7-dihydroindole is closer to the energy of the LUMO of (*E*)-(2-nitrovinyl)benzene. Therefore the higher HOMO energy of 4,7-dihydroindole may account for its higher reactivity in the Friedel–Crafts reaction.[18] In addition, the structure of the transition state may also affect the energy barriers. There is a small difference between the nucleophile-attacking angle to the nitroolefin in **TS-A** and **TS-B** (Fig. 4). The angle A(C1–C2–C5) in **TS-A** is 109.9°, 3° smaller than A(C4–C2–C5) in **TS-B** (112.9°). The 4,7-dihydroindole attacks the nitroolefin in a direction closer to Dünitz angle (105±5°), the favorite trajectory for a nucleophile to attack a sp^2 carbon atom.[19] This difference should be caused by the different ring sizes in **TS-A** and **TS-B**. In the larger 12-membered transition state **TS-B**, the constraint of the cyclic structure inevitably lead to a larger attacking angle.

The regioselectivities between the 2- and 3-position of indole and 4,7-dihydroindole in the Friedel–Crafts reaction were also investigated. As expected, the 2-position of 4,7-dihydroindole and the 3-position of indole are the more active reaction sites. The energy barrier of the nucleophilic attacking at 2-position of 4,7-dihydroindole was 7.0 kcal/mol lower than that at 3-position. The corresponding energetic gap of indole was 7.3 kcal/mol (Fig. 5).

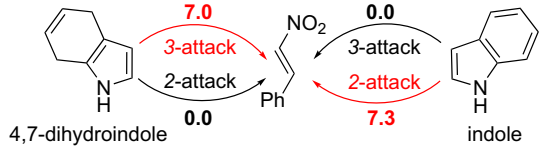

Figure 5. The relative energetic barriers of nucleophilic attacking at different position of 4,7-dihydroindole and indole. The relative Gibbs free energies in gas phase (ΔG_{gas}) are in kcal/mol. Calculated on B3LYP/6-31G(d, p) level of theory.

3.3. Understanding the origin of the enantioselectivity

In order to understand the origin of the enantioselectivity of the Friedel–Crafts reactions between 4,7-dihydroindoles and nitroolefins, calculations were performed with complete models using chiral phosphoric acid catalyst (*S*)-**1c**. After an exhausted conformational search, 16 distinct transition states to both enantiomers have been located in gas phase using PBE1PBE functional and 6-31G(d, p) basis set (Fig. 6). Frequency analyses were carried out for the six most stable transition states.

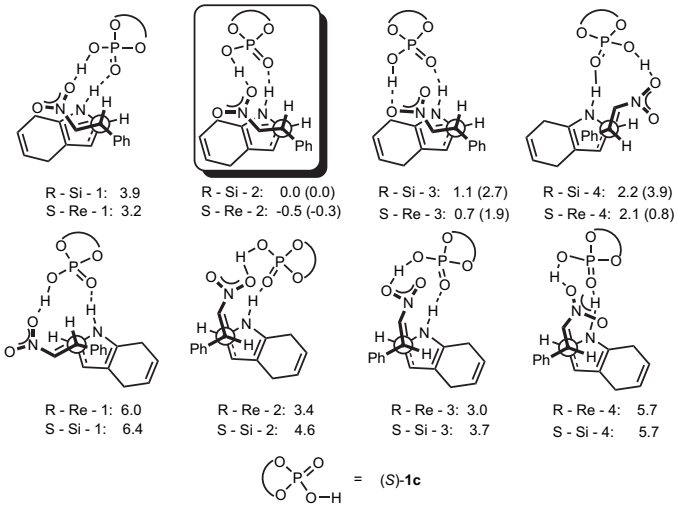

Figure 6. Newman projections of all possible transition states. ΔE_{gas} and ΔG_{gas} (in parentheses) are in kcal/mol. Calculated at PBE1PBE/6-31G(d, p) level of theory.

The relative electronic energies (ΔE_{gas}) of these transition states are quite diverse (Fig. 6). Take the eight transition states affording (*R*)-product as example, the energy difference between the most unstable and the most stable transition state is 6.0 kcal/mol. The 4,7-dihydroindole preferentially attacks the *Re*-face of nitroolefin with its *Si*-face. The energies of ***R*–*Si*–n** are about 3 kcal/mol lower than that of ***R*–*Re*–n**. Similar trend could be observed for the transition state series that accessed to the (*S*)-product. Among these structures, ***R*–*Si*–2** and its diastereomeric counterpart ***S*–*Re*–2** are the most favorite transition states leading to (*R*)- and (*S*)-product, respectively. Both of them have minimized repulsion between the two substrates and meanwhile maintain suitable orientation for hydrogen bonding.

In order to get more accurate energies, the six most stable transition states with catalyst (*S*)-**1c** were reoptimized using PBE1PBE method (the model shown in Fig. 1-B). In these models, the two substrates and the '*core*' part of the catalysts ($O_2P(=O)OH$) were described by 6-311+G(d, p) basis set, the BINOL skeleton and the bulky R groups were described by 6-31G(d, p) basis set. Frequency analyses were then performed and solvent effects were considered using the IEFPCM model (UAHF radii) in dichloromethane (ε=8.93). The results are summarized in Table 1. The structures of ***R*–*Si*–2**$_{(9\text{-anthryl})}$ and ***S*–*Re*–2**$_{(9\text{-anthryl})}$ are shown in Figure 7.

Table 1
The calculated relative energies of the six most stable transition states with catalyst (*S*)-**1c** on PBE1PBE/[6-311+G(d,p), 6-31G(d,p)] level of theory. All energies are in kcal/mol, *T*=298.15 K

TS	ΔE_{gas}	$-T\Delta S$	ΔG_{gas}	ΔG_{corr}	ΔG_{sol}
***R*–*Si*–2**$_{(9\text{-anthryl})}$	**0.0**	**0.0**	**0.0**	**0.0**	**0.0**
***R*–*Si*–3**$_{(9\text{-anthryl})}$	2.6	1.1	3.7	0.4	4.1
***R*–*Si*–4**$_{(9\text{-anthryl})}$	2.0	0.5	2.2	2.1	4.3
***S*–*Re*–2**$_{(9\text{-anthryl})}$	**−0.1**	**0.1**	**−0.2**	**0.8**	**0.6**
***S*–*Re*–3**$_{(9\text{-anthryl})}$	2.2	1.2	3.2	0.6	3.8
***S*–*Re*–4**$_{(9\text{-anthryl})}$	0.7	0.1	0.2	2.9	3.1

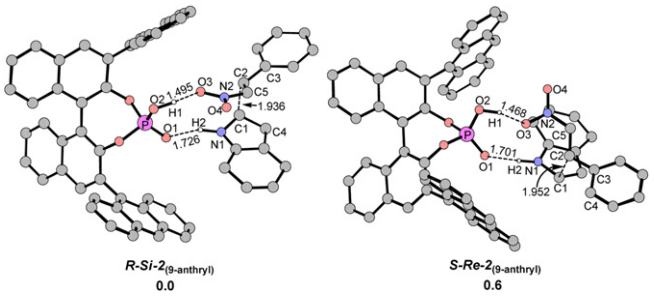

Figure 7. The optimized structures of the transition states ***R*–*Si*–2**$_{(9\text{-anthryl})}$ and ***S*–*Re*–2**$_{(9\text{-anthryl})}$. The relative Gibbs free energies including solvent effect (ΔG_{sol}) are in kcal/mol, distances are in angstroms. Calculated on PBE1PBE/[6-311+G(d,p), 6-31G(d,p)] level of theory.

As shown in Table 1, the transition states ***R*–*Si*–2**$_{(9\text{-anthryl})}$ and ***S*–*Re*–2**$_{(9\text{-anthryl})}$ are the most stable ones leading to (*R*)- and (*S*)-product, respectively. The other four structures are much unstable (more than 3 kcal/mol higher), indicating that their contributions to the ee value of the product can be omitted.

The transition states ***R*–*Si*–2**$_{(9\text{-anthryl})}$ and ***S*–*Re*–2**$_{(9\text{-anthryl})}$ have very similar structures and energies. The Gibbs free energy of ***S*–*Re*–2**$_{(9\text{-anthryl})}$ in gas phase (ΔG_{gas}) is 0.2 kcal/mol lower than that of ***R*–*Si*–2**$_{(9\text{-anthryl})}$. However, the solvent effect brings about larger discrimination to the Gibbs free energies of these two structures (ΔG_{corr}=0.8 kcal/mol), with ***R*–*Si*–2**$_{(9\text{-anthryl})}$ being the favorite one. The ΔG_{sol} suggests that the absolute configuration of the major product is *R*, which corresponds well with the experiments. Therefore, for catalyst (*S*)-**1c** the enantioselectivity is mainly determined by the solvent effect.

How does the solvation affect the enantioselectivity? The energy correction of the solvent effect ΔG_{corr} is composed of electrostatic interaction and nonelectrostatic interaction (including cavitation, dispersion, and repulsion energies).[20] A detailed comparison of these energetic terms shows that ***R*–*Si*–2**$_{(9\text{-anthryl})}$ can be better stabilized by larger electrostatic interaction with the solvent compared with ***S*–*Re*–2**$_{(9\text{-anthryl})}$ (−8.45 kcal/mol vs −7.65 kcal/mol). On the other hand, the nonelectrostatic interactions of these two structures are nearly the same (<0.1 kcal/mol in difference). Encouraged by these results, we drew the electron density surfaces of ***R*–*Si*–2**$_{(9\text{-anthryl})}$ and ***S*–*Re*–2**$_{(9\text{-anthryl})}$ based on the total density (Fig. 8). The most negatively charged region in the electron density surface is the nonactivated oxygen atom of the nitro group (red part). In ***S*–*Re*–2**$_{(9\text{-anthryl})}$, this oxygen atom is just shielded by one anthryl ring of the catalyst. Whereas in ***R*–*Si*–2**$_{(9\text{-anthryl})}$, this polarized fragment is exposed to the solvent, leading to larger electrostatic interactions. Therefore, the difference in electrostatic interactions with the solvent is caused by the different charge distributions.

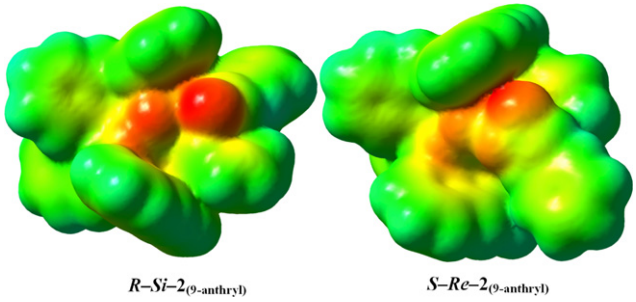

Figure 8. Electron density surfaces of ***R*–*Si*–2**$_{(9\text{-anthryl})}$ and ***S*–*Re*–2**$_{(9\text{-anthryl})}$ based on the total density. Red: negative charge; Blue: positive charge; Green: neutral.

Subsequently, the enantioselectivity of the Friedel–Crafts reactions between 4,7-dihydroindoles and nitroolefins with catalyst (*S*)-**1b** was studied. Based on the previous calculations, only the two most stable transition states ***R*–*Si*–2**$_{(SiPh3)}$ and ***S*–*Re*–2**$_{(SiPh3)}$ were considered. The results are summarized in Table 2.

Table 2
The calculated relative energies of the two most stable transition states with catalyst (*S*)-**1b** on PBE1PBE/[6-311+G(d, p), 6-31G(d, p)] level of theory. All energies are in kcal/mol, *T*=298.15 K

TS	ΔE_{gas}	$-T\Delta S$	ΔG_{gas}	ΔG_{corr}	ΔG_{sol}
***R*–*Si*–2**$_{(SiPh3)}$	0.7	0.3	1.4	−0.1	1.3
***S*–*Re*–2**$_{(SiPh3)}$	0.0	0.0	0.0	0.0	0.0

Quite different from catalyst (*S*)-**1c**, for (*S*)-**1b**, ***S*–*Re*–2**$_{(SiPh3)}$ becomes the more stable transition state, whose Gibbs free energy is 1.3 kcal/mol lower than that of ***R*–*Si*–2**$_{(SiPh3)}$. Thus the absolute configuration of the major product switches to *S*, which is consistent well with the experiment. As shown in Figure 9, in ***R*–*Si*–2**$_{(SiPh3)}$, the 4,7-dihydroindole is very close to one phenyl ring of the left $SiPh_3$ group, which would cause stronger repulsion than that in ***S*–*Re*–2**$_{(SiPh3)}$. Meanwhile, the more congested structure of ***R*–*Si*–2**$_{(SiPh3)}$ is also unfavorable in terms of entropy (the contribution of ΔS to the Gibbs free energy for ***R*–*Si*–2**$_{(SiPh3)}$ is 0.3 kcal/mol). The difference of the solvent effect (ΔG_{corr}) of these two transition states is only 0.1 kcal/mol, and the electron density surfaces also do not show obvious distinction in charge distribution (Fig. 10). In this system the enantioselectivity is determined by the steric effect.

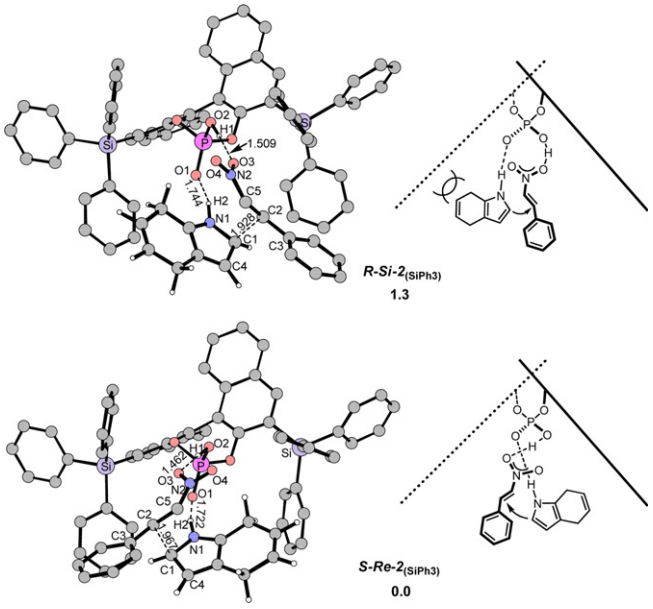

Figure 9. The optimized structures of the transition states ***R*–*Si*–2**$_{(SiPh3)}$ and ***S*–*Re*–2**$_{(SiPh3)}$ Selected hydrogen atoms are omitted for clarity. The relative Gibbs free energies including solvent effrct (ΔG_{sol}) are in kcal/mol, distances are in angstroms. Calculated on PBE1PBE/[6-311+G(d, p), 6-31G(d, p)] level of theory.

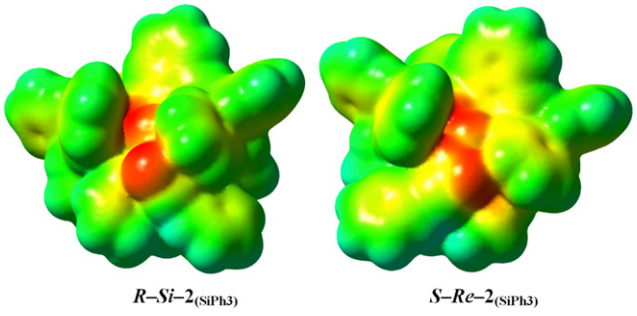

Figure 10. Electron density surfaces of ***R*–*Si*–2**$_{(SiPh3)}$ and ***S*–*Re*–2**$_{(SiPh3)}$ based on the total density. Red: negative charge; Blue: positive charge; Green: neutral.

Finally, one crucial question remains to be answered is why the predominant factors that determine the overall enantioselectivities are different in two very similar catalytic systems? We believe that in the system of (*S*)-**1b** the two $SiPh_3$ groups provide more complete reaction pocket that embraces the substrates better, avoiding external solvent effects. Thus the enantioselectivity of the reaction is entirely controlled by the chiral discrimination to the transition states of the catalyst itself. Given that Akiyama used (*R*)-**1a** in the indole system to afford (*R*)-product, it is reasonable that in our system the catalyst (*S*)-**1b** affords (*S*)-product with 4,7-dihydroindole as the nucleophile. However, the bulky substitution 9-anthryl is less steric-demanding than $SiPh_3$. Direct interactions between 9-anthryl and the substrates should be diminished, giving nearly identical ΔG_{gas} for transition states accessing both enantiomeric products. The relatively less shielded transition state structures permit more remarkable solvent effects to the whole systems, and the enantioselectivity originates from this 'external' discrimination eventually.[21]

4. Conclusion

In summary, density functional theory calculations have been carried out on chiral phosphoric acid-catalyzed Friedel–Crafts reaction of nitroolefin with 4,7-dihydrodindole/indole. 4,7-Dihydroindole is more nucleophilic than indole in the view of frontier molecular orbital energies. Besides, the 11-membered ring transition structure also contributes to its high reactivity.

The reversal of the enantioselectivies in the Friedel–Crafts reaction of 4,7-dihydroindole and nitroolefin caused by switch of 3,3′-substituted groups was explained qualitatively. When the catalyst (*S*)-**1b** was used, the transition state leading to (*R*)-product suffered from slightly stronger repulsion between the 4,7-dihydroindole and one $SiPh_3$ group of the catalyst, which results in the moderate enantiomeric excess (*S*) observed experimentally. Whereas for catalyst (*S*)-**1c**, the different solvent effects of the two transition states became predominant, products of opposite configuration (*R*) were obtained with high ees.

Acknowledgements

We thank the National Natural Science Foundation of China (20732006, 20821002, 20872168, 20932008), National Basic Research Program of China (973 Program 2009CB825300) for generous financial support.

Supplementary data

Supplementary data associated with this article can be found in online version at doi:10.1016/j.tet.2010.02.031.

References and notes

1. Reviews on chiral phosphoric-acid catalysis: (a) Taylor, M. S.; Jacobsen, E. N. *Angew. Chem., Int. Ed.* **2006**, *45*, 1520; (b) Akiyama, T.; Itoh, J.; Fuchibe, K. *Adv. Synth. Catal.* **2006**, *348*, 999; (c) Connon, S. J. *Angew. Chem., Int. Ed.* **2006**, *45*, 3909; (d) Akiyama, T. *Chem. Rev.* **2007**, *107*, 5744; (e) Yu, X.; Wang, W. *Chem. Asian J.* **2008**, *3*, 516; (f) Terada, M. *Chem. Commun.* **2008**, 4097.
2. For selected examples: (a) Akiyama, T.; Itoh, J.; Yokota, K.; Fuchibe, K. *Angew. Chem., Int. Ed.* **2004**, *43*, 1566; (b) Uraguchi, D.; Terada, M. *J. Am. Chem. Soc.* **2004**, *126*, 5356; (c) Guo, Q.-X.; Liu, H.; Guo, C.; Luo, S.-W.; Gu, Y.; Gong, L.-Z. *J. Am. Chem. Soc.* **2007**, *129*, 3790; (d) Rueping, M.; Sugiono, E.; Schoepke, F. R. *Synlett* **2007**, 1441; (e) Gridnev, I. D.; Kouchi, M.; Sorimachi, K.; Terada, M. *Tetrahedron Lett.* **2007**, *48*, 497; (f) Itoh, J.; Fuchibe, K.; Akiyama, T. *Synthesis* **2008**, 1319.
3. For selected examples: (a) Uraguchi, D.; Sorimachi, K.; Terada, M. *J. Am. Chem. Soc.* **2004**, *126*, 11804; (b) Jia, Y.-X.; Zhong, J.; Zhu, S.-F.; Zhang, C.-M.; Zhou, Q.-L. *Angew. Chem., Int. Ed.* **2007**, *46*, 5565; (c) Terada, M.; Sorimachi, K. *J. Am. Chem. Soc.* **2007**, *129*, 292; (d) Kang, Q.; Zhao, Z.-A.; You, S.-L. *J. Am. Chem. Soc.* **2007**, *129*, 1484; (e) Terada, M.; Yokoyama, S.; Sorimachi, K.; Uraguchi, D. *Adv. Synth. Catal.* **2007**, *349*, 1863; (f) Rowland, G. B.; Rowland, E. B.; Liang, Y.; Perman, J. A.; Antilla, J. C. *Org. Lett.* **2007**, *9*, 2609; (g) Li, G.; Rowland, G. B.; Rowland, E. B.; Antilla, J. C. *Org. Lett.* **2007**, *9*, 4065; (h) Itoh, J.; Fuchibe, K.; Akiyama, T. *Angew. Chem., Int. Ed.* **2008**, *47*, 4016; (i) Kang, Q.; Zheng, X.-J.; You, S.-L. *Chem.—Eur. J.* **2008**, *14*, 3539; (j) Sheng, Y.-F.; Li, G.-Q.; Kang, Q.; Zhang, A.-J.; You, S.-L. *Chem.—Eur. J.* **2009**, *15*, 3351; (k) Kang, Q.; Zhao, Z.-A.; You, S.-L. *Tetrahedron* **2009**, *65*, 1603; (l) Sun, F.-L.; Zeng, M.; Gu, Q.; You, S.-L. *Chem.—Eur. J.* **2009**, *15*, 8709.
4. For selected examples: (a) Hoffmann, S.; Seayad, A. M.; List, B. *Angew. Chem., Int. Ed.* **2005**, *44*, 7424; (b) Rueping, M.; Sugiono, E.; Azap, C.; Theissmann, T.; Bolte, M. *Org. Lett.* **2005**, *7*, 3781; (c) Rueping, M.; Antonchich, A. P.; Theissmann, T. *Angew. Chem., Int. Ed.* **2006**, *45*, 3683; (d) Rueping, M.; Antonchich, A. P.; Theissmann, T. *Angew. Chem., Int. Ed.* **2006**, *45*, 6751; (e) Rueping, M.; Antonchich, A. P. *Angew. Chem., Int. Ed.* **2007**, *46*, 4562; (f) Li, G.; Liang, Y.; Antilla, J. C. *J. Am. Chem. Soc.* **2007**, *129*, 5830; (g) Zhou, J.; List, B. *J. Am. Chem. Soc.* **2007**, *129*, 7498; (h) Kang, Q.; Zhao, Z.-A.; You, S.-L. *Adv. Synth. Catal.* **2007**, *349*, 1657; (i) Guo, Q.-S.; Du, D.-M.; Xu, J. *Angew. Chem., Int. Ed.* **2008**, *47*, 759; (j) Kang, Q.; Zhao, Z.-A.; You, S.-L. *Org. Lett.* **2008**, *10*, 2031.
5. For selected examples: (a) Itoh, J.; Fuchibe, K.; Akiyama, T. *Angew. Chem., Int. Ed.* **2006**, *45*, 4796; (b) Akiyama, T.; Morita, H.; Fuchibe, K. *J. Am. Chem. Soc.* **2006**, *128*, 13070; (c) Liu, H.; Cun, L.-F.; Mi, A.-Q.; Jiang, Y.-Z.; Gong, L.-Z. *Org. Lett.* **2006**, *8*, 6023; (d) Akiyama, T.; Tamura, Y.; Itoh, J.; Morita, H.; Fuchibe, K. *Synlett* **2006**, 141; (e) Gioia, C.; Hauville, A.; Bernardi, L.; Fini, F.; Ricci, A. *Angew. Chem., Int. Ed.* **2008**, *47*, 9236.
6. For selected examples: (a) Chen, X.-H.; Xu, X.-Y.; Liu, H.; Cun, L.-F.; Gong, L.-Z. *J. Am. Chem. Soc.* **2006**, *128*, 14082; (b) Li, N.; Chen, X.-H.; Song, J.; Luo, S.-W.; Fan, W.; Gong, L.-Z. *J. Am. Chem. Soc.* **2009**, *131*, 15301; (c) Akiyama, T.; Katoh, T.; Mori, K. *Angew. Chem., Int. Ed.* **2009**, *48*, 4226.
7. For selected examples: (a) Komanduri, V.; Krische, M. J. *J. Am. Chem. Soc.* **2006**, *128*, 16448; (b) Hamilton, G. L.; Kang, E. J.; Mba, M.; Toste, F. D. *Science* **2007**, *317*, 496; (c) Rueping, M.; Antonchick, A. P.; Brinkmann, C. *Angew. Chem., Int. Ed.* **2007**, *46*, 6903; (d) Mukherjee, S.; List, B. *J. Am. Chem. Soc.* **2007**, *129*, 11336; (e) Hu, W.-H.; Xu, X.-F.; Zhou, J.; Liu, W.-J.; Huang, H.-X.; Hu, J.; Yang, L.-P.; Gong, L.-Z. *J. Am. Chem. Soc.* **2008**, *130*, 7782; (f) Li, C.-Q.; Wang, C.; Villa-Marcos, B.; Xiao, J.-L. *J. Am. Chem. Soc.* **2008**, *130*, 14450; (g) Li, C.-Q.; Wang, C.; Villa-Marcos, B.; Xiao, J.-L. J. *Am. Chem. Soc.* **2009**, *131*, 6967; (h) Sorimachi, K.; Terada, M. *J. Am. Chem. Soc.* **2008**, *130*, 14452; (i) Terada, M.; Toda, Y. *J. Am. Chem. Soc.* **2009**, *131*, 6354; (j) Muratore, M. E.; Holloway, C. A.; Pilling, A. W.; Storer, R. I.; Trevitt, G.; Dixon, D. J. *J. Am. Chem. Soc.* **2009**, *131*, 10796; (k) Cai, Q.; Zhao, Z.-A.; You, S.-L. *Angew. Chem., Int. Ed.* **2009**, *48*, 7428; (l) Zhang, Q.-W.; Fan, C.-A.; Zhang, H.-J.; Tu, Y.-Q.; Zhao, Y.-M.; Gu, P.; Chen, Z.-M. *Angew. Chem., Int. Ed.* **2009**, *48*, 8572; (m) Liu, X.-Y.; Che, C.-M. *Org. Lett.* **2009**, *11*, 4204.
8. (a) Yamanaka, M.; Itoh, J.; Fuchibe, K.; Akiyama, T. *J. Am. Chem. Soc.* **2007**, *129*, 6756; (b) Simón, L.; Goodmann, J. M. *J. Am. Chem. Soc.* **2008**, *130*, 8741; (c) Simón, L.; Goodmann, J. M. *J. Am. Chem. Soc.* **2009**, *131*, 4070; (d) Marcelli, T.; Hammar, P.; Himo, F. *Chem.—Eur. J.* **2008**, *14*, 8562; (e) Marcelli, T.; Hammar, P.; Himo, F. *Adv. Synth. Catal.* **2009**, *351*, 525; (f) Yamanaka, M.; Hirata, T. *J. Org. Chem.* **2009**, *74*, 3266; (g) Shi, F.-Q.; Song, B.-A. *Org. Biomol. Chem.* **2009**, *7*, 1292; (h) Xu, S.; Wang, Z.; Li, Y.; Zhang, X.; Wang, H.; Ding, K. *Chem.—Eur. J.*, in press. doi:10.1002/chem.200902698
9. For reviews on asymmetric Friedel–Crafts reactions: (a) Bandini, M.; Melloni, A.; Umani-Ronchi, A. *Angew. Chem., Int. Ed.* **2004**, *43*, 550; (b) Bandini, M.; Melloni, A.; Tommasi, S.; Umani-Ronchi, A. *Synlett* **2005**, 1199; (c) Poulsen, T. B.; Jørgensen, K. A. *Chem. Rev.* **2008**, *108*, 2903; (d) You, S.-L.; Cai, Q.; Zeng, M. *Chem. Soc. Rev.* **2009**, *38*, 2190. After the acceptance of this manuscript, Goodman et al. reported an excellent theoretical investigation into chiral phosphoric acid-catalyzed Friedel–Crafts reactions of various imines; (e) Simón, L.; Goodman, J. M. *J. Org. Chem.* **2010**, *75*, 589.
10. For other literature reports in which the configuration of the final products could be switched in chiral phosphoric-acid catalysis caused only by changes of 3,3′-substitution group on the catalyst, please see: Ref. 2b,3e,4e,j,6a,b and Wanner, M. J.; van der Haas, R. N. S.; de Cuba, K. R.; van Maarseveen, J. H.; Hiemstra, H. *Angew. Chem., Int. Ed.* **2007**, *46*, 7485.
11. Frisch, M. J.; Trucks, G. W.; Schlegel, H. B.; Scuseria, G. E.; Robb, M. A.; Cheeseman, J. R.; Montgomery, J. J. A.; Vreven, T.; Kudin, K. N.; Burant, J. C.; Millam, J. M.; Iyengar, S. S.; Tomasi, J.; Barone, V.; Mennucci, B.; Cossi, M.; Scalmani, G.; Rega, N.; Petersson, G. A.; Nakatsuji, H.; Hada, M.; Ehara, M.; Toyota, K.; Fukuda, R.; Hasegawa, J.; Ishida, M.; Nakajima, T.; Honda, Y.; Kitao, O.; Nakai, H.; Klene, M.; Li, X.; Knox, J. E.; Hratchian, H. P.; Cross, J. B.; Bakken, V.; Adamo, C.; Jaramillo, J.; Gomperts, R.; Stratmann, R. E.; Yazyev, O.; Austin, A. J.; Cammi, R.; Pomelli, C.; Ochterski, J. W.; Ayala, P. Y.; Morokuma, K.; Voth, G. A.; Salvador, P.; Dannenberg, J. J.; Zakrzewski, V. G.; Dapprich, S.; Daniels, A. D.; Strain, M. C.; Farkas, O.; Malick, D. K.; Rabuck, A. D.; Raghavachari, K.; Foresman, J. B.; Ortiz, J. V.; Cui, Q.; Baboul, A. G.; Clifford, S.; Cioslowski, J.; Stefanov, B. B.; Liu, G.; Liashenko, A.; Piskorz, P.; Komaromi, I.; Martin, R. L.; Fox, D. J.; Keith, T.; Al-Laham, M. A.; Peng, C. Y.; Nanayakkara, A.; Challacombe, M.; Gill, P. M. W.; Johnson, B.; Chen, W.; Wong, M. W.; Gonzalez, C.; Pople, J. A. *Gaussian 03 (Revision D.01)*; Gaussian: Wallingford, CT, 2004.
12. (a) Lee, C.; Yang, W.; Parr, R. G. *Phys. Rev. B* **1988**, *37*, 785; (b) Becke, A. D. *Phys. Rev. A* **1988**, *38*, 3098; (c) Becke, A. D. *J. Chem. Phys.* **1992**, *96*, 2155; (d) Becke, A. D. *J. Chem. Phys.* **1992**, *97*, 9173; (e) Becke, A. D. *J. Chem. Phys.* **1993**, *98*, 5648.
13. (a) Perdew, J. P.; Burke, K.; Ernzerhof, M. *Phys. Rev. Lett.* **1996**, *77*, 3865; (b) Perdew, J. P.; Burke, K.; Ernzerhof, M. *Phys. Rev. Lett.* **1997**, *78*, 1396.
14. Zhao, Y.; Truhlar, D. G. *J. Chem. Theory Comput.* **2005**, *1*, 415.
15. (a) Cances, M. T.; Mennucci, V.; Tomasi, J. *J. Chem. Phys.* **1997**, *107*, 3032; (b) Cossi, M.; Barone, V.; Tomasi, J. *J. Phys., Lett.* **1998**, *286*, 253.
16. Chiral phosphoric acids used in the activation of carbonyl compounds, see: Ref. 6c and (a) Rueping, M.; Ieawsuwan, W.; Antonchick, A. P.; Nachtsheim, B. J.

Angew. Chem., Int. Ed. **2007**, *46*, 2097; (b) Terada, M.; Soga, K.; Momiyama, N. *Angew. Chem., Int. Ed.* **2008**, *47*, 4122.
17. Smith, M. B.; March, J. *March's Advanced Organic Chemistry*, 5th ed.; Wiley: New York, NY, 2000; pp 675–681.
18. (a) Carey, F. A.; Sundberg, R. J. *Advanced Organic Chemistry*, 4th ed.; Kluwer: New York, NY, 2000; pp 568–571; (b) Pearson, R. G. *Proc. Natl. Acad. Sci. U.S.A.* **1986**, *83*, 8440; (c) Zhou, Z.; Parr, R. G. *J. Am. Chem. Soc.* **1990**, *112*, 5720.
19. Bürgi, H. B.; Dünitz, J. D.; Lehn, J. M.; Wipff, G. *Tetrahedron* **1974**, *30*, 1563.
20. (a) Ben-Naim, A. *Water and Aqueous Solutions*; Plenum: New York, NY, 1974; (b) Ben-Naim, A. *J. Phys. Chem.* **1978**, *82*, 792; (c) Ben-Naim, A. *Solvation Thermodinamics*; Plenum: New York, NY, 1974; (d) Tomasi, J.; Persico, M. *Chem. Rev.* **1994**, *94*, 2027.
21. It has been reported that the configuration of the major product can be reversed simply by using different solvents in chiral phosphoric acid-catalyzed aza-Diels–Alder reaction, see Ref. 5d.